When a red NIR emissive Cs2[Mo6Br14] interacts with an active diureasil-PEO matrix design of tunable and white light emitting hybrid material

Eduardo Ferreira Molina, Natana Aparecida Martins de Jesus, Serge Paofai, Peter Hammer, Maria Amela-Cortes, Malo Robin, Stéphane Cordier, Yann Molard

▶ To cite this version:

Eduardo Ferreira Molina, Natana Aparecida Martins de Jesus, Serge Paofai, Peter Hammer, Maria Amela-Cortes, et al.. When a red NIR emissive Cs2[Mo6Br14] interacts with an active diureasil-PEO matrix design of tunable and white light emitting hybrid material. Chemistry - A European Journal, 2019, 25 (67), pp.15248-15251. 10.1002/chem.201903892 . hal-02307028

HAL Id: hal-02307028
https://univ-rennes.hal.science/hal-02307028

Submitted on 21 Feb 2020

When a red NIR emissive Cs$_2$[Mo$_6$Br$_{14}$] interacts with an active diureasil-PEO matrix: design of tunable and white light emitting hybrid material.

Eduardo Ferreira Molina,[a]* Natana Aparecida Martins de Jesus,[a] Serge Paofai,[b] Peter Hammer,[c] Maria Amela-Cortes,[b] Malo Robin,[b] Stephane Cordier[b] and Yann Molard[b]*

Hybrid materials combining diureasil matrices and octahedral molybdenum clusters have been synthesized to design lead-, cadmium and rare earth-free emitters for lighting or optoelectronic applications. This association leads to homogeneous and stable hybrids which emission color can be tailored on the entire visible range, including white, thanks to effective energy transfers from the host to the nanocluster.

Transition metal cluster compounds are based on a metal atoms scaffold maintained by metal-metal bonds.[1] In the field of luminescent materials, octahedral clusters made of low cost and abundant metals like Mo or W, constitute attractive alternatives to toxic cadmium- or lead-, costly Ir(III)-, Pt(II)- or rare earth – containing luminophores.[2] Recent developments in this area have highlighted their potential in optoelectronic,[3] sensing,[4] lighting,[5] theranostic,[6] luminescent solar concentrators,[7] or photocatalysis.[8] Due to their high emission stability in the red-NIR,[5, 9] they show a great potential for lighting technologies to design white light emission panels. White light emission involves usually the combination of three (blue, green and red) complementary emitters, which requires tedious multilayer devices engineering. One possibility to tackle this problem is to gather all emitters in a single material and this, in a one-pot reaction. To succeed, the host matrix should be judiciously chosen in terms of thermal and photostability while being chemically compatible to circumvent phase segregation between organic and inorganic components.[10] Furthermore, it should also be able to maintain the initial photophysical properties of native dyes after their integration.[11] Diureasils[12] are hybrid materials belonging to the Ormocer® family.[13] They contain siliceous domains connected, *via* urea linkers, to poly(ethylene oxide)/poly(propylene oxide) (PEO/PPO) chains that provide distinct hydrophilic, swelling, mechanical and optical properties. Electron-hole radiative recombinations in both the siliceous and urea-centered domains,[14] [15] evidence that such matrix can act as active host for various luminophores like organic dyes,[16] lanthanide complexes,[17] quantum dots[18] or conjugated polymers.[19] Recently, we have shown that supramolecular interactions between PEO chains and alkali cations could be used to incorporate alkali salts of metal clusters in organic polymers.[5] Motivated by these results, we postulated that a blue-green emissive ureasil matrix could easily be associated with red NIR emissive alkali salts of metal clusters. Here we present the synthesis of molybdenum cluster compounds incorporated in the diureasil hybrid, named **dUPEO**, and show that molybdenum clusters can be homogeneously integrated using the diureasil sol-gel process. We demonstrate that the **dUPEO** hybrid matrix has a great potential in practical use as a solid-state luminescence device providing a tunable emissive material in which the emission color can be judiciously controlled by varying the Mo$_6$ cluster content and/or the excitation wavelength.

Figure 1 presents the molecular structure of the **dUPEO** precursors and the **Cs$_2$Mo$_6$Br$_{14}$** metal cluster salt (**1**) used as a cluster compound model due to its simple synthesis, and stability.[20] Two synthetic schemes were followed: the first one depicts the mixing of different amounts of **1** and PEO hybrid sol before the hydrolysis reaction leading to cross-linking of ureasil nodes (**E1** - **E5** samples). This synthesis route allows a facile preparation of **dUPEO** containing different amounts of **1** (see amount wt% in **Table 1**). The second scheme refers to the formation of monolithic xerogels (**dUPEO**) followed by the cluster adsorption in solution (named **CA** sample). In this latter case, the cluster concentration within **CA** was estimated by UV-Vis spectroscopy to be around 1 wt% (see Electronic Supplementary Information (**ESI**) and **Figure S1**). Cluster loading concentrations and properties of hybrids are summarized in **Table 1**. Both methods lead to homogeneous and transparent monoliths as shown in **Figure 1**. The samples were first characterized by differential scanning calorimetry and small angle X-ray scattering (see **ESI TableS1** and **Figure S2-S8** for DSC thermograms and interpretation and **Figure S9** for SAXS patterns). In the latter case, we noticed that **1** alters the average correlation distance between the ureasil crosslinking nodes (ξ_d) from 48 Å for **dUPEO** to 43 Å for **E2** and **E3**. This indicates a small contraction of the polymeric structure and suggests interactions between **1** and the urea or ether groups present in the xerogel, in good accordance with FTIR spectroscopy analysis (see **ESI Figures S10-S12**). At low q-values the contribution of **1** is observed, which arises from the high electron density contrast between clusters and matrix. A broad peak centered at ~0.35 nm^{-1} evidences inter-clusters

---

[a] Dr. E. Ferreira Molina, N. A. Martins de Jesus,
Universidade de Franca,
Av. Dr. Armando Salles Oliveira 201, 14404-600 Franca, SP, Brazil
E-mail: Eduardo.molina@unifran.edu.br

[b] S. Paofai, Dr. M. Amela-Cortes, Dr. M. Robin, Dr. S. Cordier, Dr. Y. Molard,
Univ Rennes, CNRS, ISCR - UMR 6226, ScanMAT – UMS 2001, F-35000 Rennes, France
E-mail : yann.molard@univ-rennes1.fr

[c] Dr. P. Hammer
Instituto de Quimica, UNESP-Universidade Estadual Paulista,
4800-900, Araraquara, SP, Brazil

Supporting information for this article is given via a link at the end of the document.

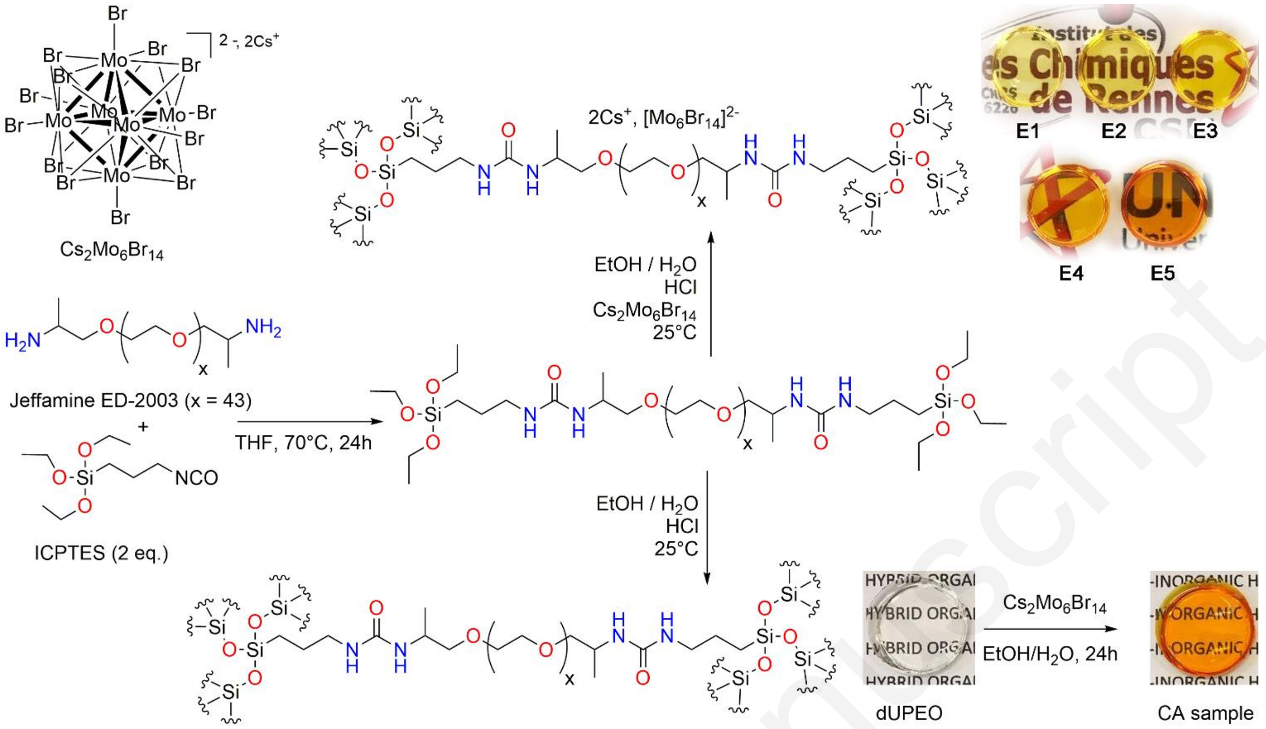

Figure 1. Structure of octahedral $Cs_2Mo_6Br_{14}$ metal cluster compound (**1**), diureasil PEO (dUPEO) hybrid sol and synthetic schemes for the preparation of unloaded and loaded dUPEO xerogel containing **1**.

interactions, due to the coexistence of dense aggregates. The distribution of **1** within the most loaded xerogel matrices, namely **E4** and **E5**, was further investigated by X-ray fluorescence spectroscopy (see ESI **Figure S13-14**) and X-ray photoelectron spectroscopy (see ESI, **Table S2** and **Figure S15**). The microanalysis reveals that **1** is well dispersed at the macroscopic level. However, the appearance of Mo and Br hotspots of tens of micrometers highlights that, at the microscopic level, the cluster distribution is not completely homogenous, in good accordance with SAXS measurements. The elemental composition of the near surface region (< 5 nm) of the loaded samples was obtained from the intensities of XPS high-resolution spectra. Within the experimental error of ±5%, the hybrids composition was close to the nominal concentration of elements. Interestingly, the signal corresponding to the nitrogen content of the xerogel matrix was reduced by a factor 2 after the incorporation of **1**. This attenuation is assessed to the interaction of clusters with urea groups. Fitted Cs $3d_{5/2}$, Br 3d and Mo 3d spectra of crystalline **1** salt reference and N 1s of pure dUPEO were compared with those recorded for **E5**. The two cesium components fitted for **1** correspond to the two crystallographic positions of Cs^+ within the single crystal structure and are located at 724.3 eV and 725.0 eV, respectively. After incorporation into **dUPEO**, only one component located at 724.3 eV was detected with a about 0.2 eV reduced peak width (FWHM), indicative of the equivalence of Cs^+ cations. The fitted N 1s spectrum of **dUPEO** shows a main component, related to the urea group at 399.7 eV, and a small sub-peak (~15% peak area) at a binding energy of 401.5 eV, attributed to a group of positively charged nitrogen. The disappearance of the small $–N^+$ component for the loaded **dUPEO** hybrid hints on an interaction between the $[Mo_6Br_{14}]^{2-}$ anion with the urea group. This corroborates well with the attenuation of nitrogen content observed once **dUPEO** is loaded. Hence, the protonated urea located at the surface of the silica nodes are acting as cluster counter cations. These electrostatic interactions being stronger than those occurring between Cs^+ and PEO chains, it explains the inhomogeneity observed by µ-X-ray fluorescence spectroscopy at the microscopic level.

Emission properties were investigated by steady state and time resolved experiments. To assess about the hybrids stability, photophysical characterizations were realized twice with a time interval of 48 months. Similar results were obtained in both cases.

Table 1. Glass transition temperature, T_g, cluster content, kinetic parameters and absolute quantum yield (AQY) of prepared hybrids.

	T_g (°C)	**1** (wt%)	Kinetic parameters		AQY[b]	
			ureasil range τ_{av}/ ns [a]	Cluster range τ_{av} / µs [a]	Air	N_2
dUPEO	-58.3	0	6.0	-	0.18	-
E1	-55.5	0.1	4.7	66.7	0.09	0.12
E2	-51.7	0.5	4.1	44.7	0.07	0.12
E3	-49.7	1	3.6	49.4	0.07	0.12
E4	-48.1	3	-	37.6	0.06	0.17
E5	-31.1	10	-	30.2	0.05	0.15
CA	-51.3	~1	1.9	42.9	0.04	0.14

[a] $\tau_{av} = (\Sigma a_i \tau_i^2)/(\Sigma a_i \tau_i)$; [b] error on values is estimated at ±10%

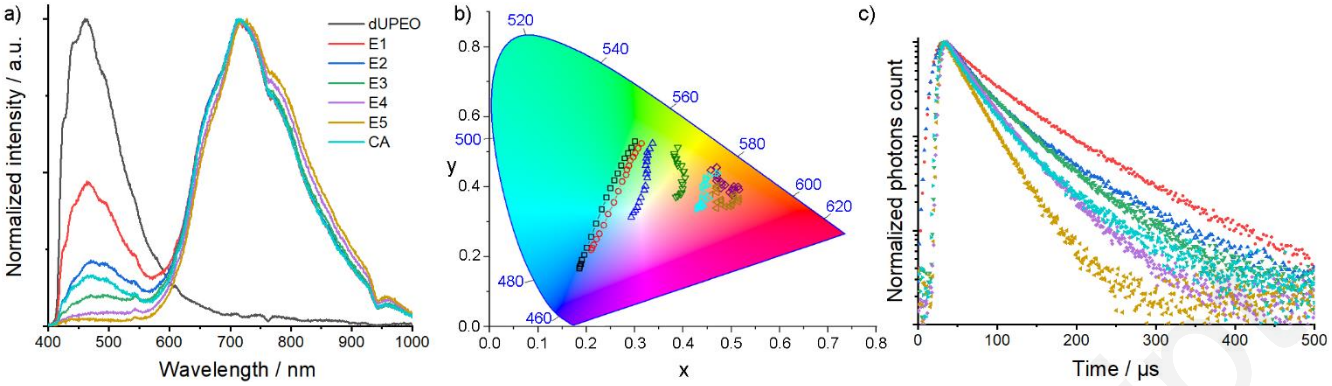

Figure 2.a) Normalized emission spectra of hybrid materials irradiated between 350-380 nm; b) CIE 1938 diagram coordinates for excitation ranging from 365 up to 450 nm: dUPEO (black), E1 (red), E2 (blue), E3 (green), E4 (purple, E5 (maroon) and CA (cyan); c) phosphorescence emission decay profiles recorded in the metal cluster emission range (662-798 nm).

Figure 2a presents the normalized emission spectra observed for all samples at λ_{exc}= 350-380 nm (see ESI, **Figure S16** for excitation *vs*. emission maps and **Figures S17 - S18** for other excitation wavelength). The emission envelope and absolute quantum yield (AQY, **Table 1**) of **dUPEO** are similar to those already reported for diureasil matrices.[14, 21] The **dUPEO** emission is ascribed to electron–hole recombination mediated by a mechanism typical of donor–acceptor pairs occurring in the urea linkages and in the oxygen-related defects in the siliceous nanodomains.[21a] Increasing the cluster load from **E1** to **E5** leads to the decrease of the blue emission and the increase of the red-NIR one. For **E4** and **E5**, the diureasil emission band is entirely quenched which indicates a quantitative energy transfer from the diureasil node to $[Mo_6Br_{14}]^{2-}$. The strong overlap between the absorption band of **1** and the **dUPEO** emission band, enables resonance energy transfers (RET) based on long-range dipole–dipole interactions in the hybrids,[22] as observed for other luminophores.[17b-d, 18-19, 23] Indeed, the Förster radius, *i.e.* the distance between emitters for which the energy transfer has a probability of 0.5, was estimated to be 4.6 nm (see ESI and **Figure S19**),[24] value close to the maximal correlation distance determined by SAXS between the diureasil cross-linking nodes. Yet, as represented on the Commission Internationale de l'Eclairage (CIE) chromaticity diagram (**Figure 2b**), the hybrid emission color can be tailored on the entire visible spectrum by judiciously adjusting the cluster concentration and the excitation wavelength. In particular, for **E2**, a white emission is observed for an excitation ranging from 365 up to 390 nm. AQY values in air were calculated for several excitations (see ESI **Figure S20**). Loading **dUPEO** with **1** decreases the emitting efficiency of the material, that is ascribed to energy losses occurring during the energy transfers, non-radiative desexcitation and quenching of cluster emission by the surrounding triplet oxygen O_2 ($^3\Sigma_g^-$).[25] In fact, saturating samples atmosphere with N_2 induces a significant increase of the AQY (Table 1 and ESI **Figure S20**) up to 300% depending on the cluster compound concentration. Time correlated emission properties were then investigated at λ_{exc}= 375 nm (see ESI **Figures S21-S38**). Two spectral ranges were observed corresponding respectively to the diureasil and to the cluster emission windows. Kinetic parameters of diureasil nodes could be recorded up to a loading concentration of 1 wt%. The diureasil emission decay was fitted using a three components exponential function as suggested by Fu *et al.*[26] However, for the ease of understanding, only average lifetime values will be considered herein (see ESI **table S3** for a full report on kinetic data). Increasing cluster content in **dUPEO** induces a decrease of **dUPEO** average lifetime value which suggests a better efficiency of the energy transfer between emitters. For the cluster emission window, emission profiles were fitted with two phosphorescent components in the tenth of microsecond scale, in line with the reported literature.[4b, 5, 6b, 9, 27] Increasing the cluster content induces a lowering of its average lifetime values (**Figure 2c**) assessed to the increased gas permeability of the host matrix that favors O_2 diffusion within the material. Indeed, it is well known that metal cluster excited triplet states[27] are efficiently quenched by triplet oxygen, and this property was already used to design oxygen sensors.[4, 25, 28]

In conclusion, highly stable organic inorganic emissive hybrids were obtained by combining **$Cs_2Mo_6Br_{14}$** with an ormocer diureasil containing poly(ethyleneoxide) chains. The homogeneity of samples is imparted to supramolecular interactions between the cluster salt Cs^+ cations and the PEO chains, and, to electrostatic interactions between the protonated urea located at the surface of silica nodes and the inorganic anions. All samples are macroscopically homogeneous up to 10 wt% doping. Steady state and lifetime emission measurements demonstrate the occurrence of an energy transfer between the blue-green emitting diureasil moieties and the red-NIR emissive clusters. This transfer becomes quantitative for cluster loads higher than 3 wt%. Hence, by an adequate choice of cluster concentration and irradiation wavelength, the emission color can be finely tuned and spread the all visible range including white, making these materials candidates of choice for optoelectronic or lighting applications.

Acknowledgements

This work was supported by the Brazilian agencies: Coordenação de Aperfeiçoamento de Pessoal de Nível Superior – (CAPES) – Finance Code 001, Conselho Nacional de Desenvolvimento Científico e Tecnológico (CNPq n° 306271/2017-6, Fundação de Amparo à Pesquisa do Estado de São Paulo (SPRINT-FAPESP grant n° 2017/50286-9), and CNRS (PRC Clustobrane 2018-2019). The authors thank Huntsman Performance Products for providing Jeffamine®, the Brazilian National Synchrotron Light Laboratory (LNLS) for his help and access to the SAXS1 beamline, and H. W. P. de Carvalho (CENA–USP) for µ-XRF analysis (EMU-FAPESP grant 2015/19121-8).

Keywords: hybrid materials • luminescence • energy transfers • metal clusters

[1] a) F. A. Cotton, *Inorg. Chem.* **1964**, *3*, 1217-1220; b) P. Braunstein, L. A. Oro, P. R. Raithby, Editors, *Metal Clusters in Chemistry, Volume 1: Molecular Metal Clusters*, Wiley, **1999**; c) R. J. Wilson, N. Lichtenberger, B. Weinert, S. Dehnen, *Chemical Reviews* **2019**, *119*, 8506-8554; d) T. Imaoka, K. Yamamoto, *Bull. Chem. Soc. Jpn.* **2019**, *92*, 941-948.

[2] a) K. Kirakci, P. Kubat, M. Dusek, K. Fejfarova, V. Sicha, J. Mosinger, K. Lang, *Eur. J. Inorg. Chem.* **2012**, 3107-3111; b) M. N. Sokolov, M. A. Mihailov, E. V. Peresypkina, K. A. Brylev, N. Kitamura, V. P. Fedin, *Dalton Trans.* **2011**, *40*, 6375-6377.

[3] a) A. Garreau, F. Massuyeau, S. Cordier, Y. Molard, E. Gautron, P. Bertoncini, E. Faulques, J. Wery, B. Humbert, A. Bulou, J.-L. Duvail, *Acs Nano* **2013**, *7*, 2977-2987; b) J. Bigeon, N. Huby, M. Amela-Cortes, Y. Molard, A. Garreau, S. Cordier, B. Bêche, J. L. Duvail, *Nanotechnology* **2016**, *27*, 255201; c) Y. Molard, *Acc. Chem. Res.* **2016**, *49*, 1514-1523.

[4] a) R. N. Ghosh, G. L. Baker, C. Ruud, D. G. Nocera, *Appl. Phys. Lett.* **1999**, *75*, 2885-2887; b) M. Amela-Cortes, S. Paofai, S. Cordier, H. Folliot, Y. Molard, *Chem. Commun.* **2015**, *51*, 8177-8180.

[5] M. Robin, N. Dumait, M. Amela-Cortes, C. Roiland, M. Harnois, E. Jacques, H. Folliot, Y. Molard, *Chem. - Eur. J.* **2018**, *24*, 4825-4829.

[6] a) A. A. Krasilnikova, M. A. Shestopalov, K. A. Brylev, I. A. Kirilova, O. P. Khripko, K. E. Zubareva, Y. I. Khripko, V. T. Podorognaya, L. V. Shestopalova, V. E. Fedorov, Y. V. Mironov, *J. Inorg. Biochem.* **2015**, *144*, 13-17; b) N. Brandhonneur, T. Hatahet, M. Amela-Cortes, Y. Molard, S. Cordier, G. Dollo, *Eur. J. Pharm. Biopharm.* **2018**, *125*, 95-105; c) K. Kirakci, J. Zelenka, M. Rumlova, J. Martincik, M. Nikl, T. Ruml, K. Lang, *J. Mater. Chem. B* **2018**, *6*, 4301-4307.

[7] Y. Zhao, R. R. Lunt, *Adv. Energy Mater.* **2013**, *3*, 1143-1148.

[8] a) A. Barras, S. Cordier, R. Boukherroub, *Appl. Catal., B* **2012**, *123-124*, 1-8; b) A. Beltran, M. Mikhailov, M. N. Sokolov, V. Perez-Laguna, A. Rezusta, M. J. Revillo, F. Galindo, *J. Mater. Chem. B* **2016**, *4*, 5975-5979; c) M. Feliz, M. Puche, P. Atienzar, P. Concepcion, S. Cordier, Y. Molard, *ChemSusChem* **2016**, *9*, 1963-1971.

[9] M. Prevot, M. Amela-Cortes, S. K. Manna, R. Lefort, S. Cordier, H. Folliot, L. Dupont, Y. Molard, *Adv. Funct. Mater.* **2015**, *25*, 4966-4975.

[10] A. C. Balazs, T. Emrick, T. P. Russell, *Science* **2006**, *314*, 1107-1110.

[11] S. Parola, B. Julián-López, L. D. Carlos, C. Sanchez, *Adv. Funct. Mater.* **2016**, *26*, 6506-6544.

[12] V. de Zea Bermudez, L. D. Carlos, L. Alcácer, *Chem. Mater.* **1999**, *11*, 569-580.

[13] K.-H. Haas, H. Wolter, *Curr. Opini. Solid St. M.* **1999**, *4*, 571-580.

[14] L. D. Carlos, R. A. Sá Ferreira, V. De Zea Bermudez, S. J. L. Ribeiro, *Adv. Funct. Mater.* **2001**, *11*, 111-115.

[15] T. Brankova, V. Bekiari, P. Lianos, *Chem. Mater.* **2003**, *15*, 1855-1859.

[16] a) A. Kaniyoor, B. McKenna, S. Comby, R. C. Evans, *Adv. Optic. Mater.* **2016**, *4*, 444-456; b) S. F. H. Correia, A. R. Frias, L. Fu, R. Rondão, E. Pecoraro, S. J. L. Ribeiro, P. S. André, R. A. S. Ferreira, L. D. Carlos, *Adv. Sustain. Syst.* **2018**, *2*, 1800002.

[17] a) L. D. Carlos, Y. Messaddeq, H. F. Brito, R. A. Sá Ferreira, V. de Zea Bermudez, S. J. L. Ribeiro, *Adv. Mater.* **2000**, *12*, 594-598; b) M. C. Gonçalves, V. de Zea Bermudez, R. A. Sá Ferreira, L. D. Carlos, D. Ostrovskii, J. Rocha, *Chem. Mater.* **2004**, *16*, 2530-2543; c) M. E. Mesquita, S. S. Nobre, M. Fernandes, R. A. S. Ferreira, S. C. G. Santos, M. O. Rodrigues, L. D. Carlos, V. de Zea Bermudez, *J. Photochem. Photobiol., A* **2009**, *205*, 156-160; d) M. Fang, L. Fu, R. A. S. Ferreira, L. D. Carlos, *Materials* **2018**, *11*, 2246.

[18] M. C. Neves, M. A. Martins, P. C. R. Soares-Santos, P. Rauwel, R. A. S. Ferreira, T. Monteiro, L. D. Carlos, T. Trindade, *Nanotechnology* **2008**, *19*, 155601/155601-155601/155609.

[19] a) N. Willis-Fox, A.-T. Marques, J. Arlt, U. Scherf, L. D. Carlos, H. D. Burrows, R. C. Evans, *Chem. Sci.* **2015**, *6*, 7227-7237; b) N. Willis-Fox, M. Kraft, J. Arlt, U. Scherf, R. C. Evans, *Adv. Funct. Mater.* **2016**, *26*, 532-542.

[20] K. Kirakci, S. Cordier, C. Perrin, *Z. Anorg. Allg. Chem.* **2005**, *631*, 411-416.

[21] a) L. D. Carlos, V. de Zea Bermudez, R. A. Sá Ferreira, L. Marques, M. Assunção, *Chem. Mater.* **1999**, *11*, 581-588; b) L. D. Carlos, R. A. Sá Ferreira, R. N. Pereira, M. Assunção, V. de Zea Bermudez, *J. Phys. Chem. B* **2004**, *108*, 14924-14932; c) L. F. F. F. Goncalves, C. J. R. Silva, F. K. Kanodarwala, J. A. Stride, M. R. Pereira, M. J. M. Gomes, *Mater. Chem. Phys.* **2014**, *147*, 86-94.

[22] J. R. Lakowicz, *Principles of Fluorescence Spectroscopy, third edition*, Springer, Boston, MA, **2006**.

[23] a) L. F. F. F. Goncalves, C. J. R. Silva, F. K. Kanodarwala, J. A. Stride, M. R. Pereira, M. J. M. Gomes, *Appl. Surf. Sci.* **2014**, *314*, 877-887; b) J.-J. Li, Y. Chen, J. Yu, N. Cheng, Y. Liu, *Adv. Mater.* **2017**, *29*, 1701905; c) J. Yu, Y.-M. Zhang, P.-Y. Li, Y. Liu, *Chemical Communications* **2017**, *53*, 3717-3720.

[24] P. G. Wu, L. Brand, *Anal. Biochem.* **1994**, *218*, 1-13.

[25] J. A. Jackson, C. Turro, M. D. Newsham, D. G. Nocera, *J. Phys. Chem.* **1990**, *94*, 4500-4507.

[26] L. Fu, R. A. Sá Ferreira, M. Fernandes, S. C. Nunes, V. de Zea Bermudez, G. Hungerford, J. Rocha, L. D. Carlos, *Opt. Mater.* **2008**, *30*, 1058-1064.

[27] K. Costuas, A. Garreau, A. Bulou, B. Fontaine, J. Cuny, R. Gautier, M. Mortier, Y. Molard, J.-L. Duvail, E. Faulques, S. Cordier, *Phys. Chem. Chem. Phys.* **2015**, *17*, 28574-28585.

[28] J. A. Jackson, M. D. Newsham, C. Worsham, D. G. Nocera, *Chem. Mater.* **1996**, *8*, 558-564.

Entry for the Table of Contents

COMMUNICATION

Thanks to soft interactions, metal nanoclusters and hybrid diureasil matrices can be intimately mixed to design tailored emissive materials.

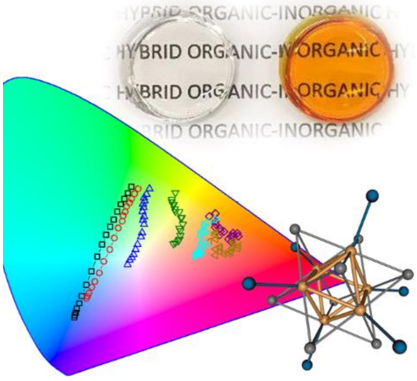

Eduardo Ferreira Molina, Natana Aparecida Martins de Jesus, Serge Paofai, Peter Hammer, Maria Amela-Cortes, Malo Robin, Stephane Cordier, Yann Molard**

Page No. – Page No.

When a red NIR emissive $Cs_2[Mo_6Br_{14}]$ interacts with an active diureasil-PEO matrix: design of tunable and white light emitting hybrid material